

**X-ray Damage to  $\text{CF}_3\text{CO}_2$ -Terminated Organic  
Monolayers on Si/Au: Principal Effect of Electrons**

PAUL E. LAIBINIS, ROBERT L. GRAHAM, HANS A. BIEBUYCK, AND GEORGE M. WHITESIDES\*

# X-ray Damage to $\text{CF}_3\text{CO}_2$ -Terminated Organic Monolayers on Si/Au: Principal Effect of Electrons

PAUL E. LAIBINIS, ROBERT L. GRAHAM, HANS A. BIEBUYCK, GEORGE M. WHITESIDES\*

The relative importance of x-rays alone and of x-ray-generated primary and secondary electrons in damaging organic materials was explored by use of self-assembled monolayers (SAMs) on multilayer thin-film supports. The substrates were prepared by the deposit of thin films of silicon (0, 50, 100, and 200 angstroms) on thick layers of gold (2000 angstroms). These systems were supported on chromium-primed silicon wafers. Trifluoroacetoxy-terminated SAMs were assembled on these substrates, and the samples were irradiated with common fluxes of monochromatic aluminum  $K_{\alpha}$  x-rays. The fluxes and energy distributions of the electrons generated by interactions of the x-rays with the various substrates, however, differed. The substrates that emitted a lower flux of electrons exhibited a slower loss of fluorine from the SAMs. This observation indicated that the electrons—and not the x-rays themselves—were largely responsible for the damage to the organic monolayer.

X-RAYS DAMAGE ORGANIC MATERIALS (1). This damage can either limit their utility or provide the basis for useful technologies such as x-ray lithography (2, 3) or radiation cross-linking of polymers (3). Understanding the mechanisms of the damage accompanying exposure to x-rays is helpful in designing materials and environments in which this exposure yields the desired results. A basic tenet of areas of technology involving x-ray processing has been that x-rays do not interact strongly with matter (4) and should effect little damage to materials. The photogenerated primary and secondary electrons interact more strongly and have been postulated to be the damaging species (5).

We and others (6) have recently begun to explore the mechanisms of x-ray-induced damage to organic materials by using SAMs on metal substrates (7–9) as samples. SAMs are well suited for this study because they allow a variety of organic functionalities to be incorporated into monomolecular films that have well-defined structures. SAMs can be easily generated that have dimensions of interest [10 to 40 Å; the characteristic escape depth (10) for electrons in the energy range encountered— $\leq 1.5$  keV—is 20 to 40 Å]. Various substrates can be derivatized with different types of SAMs: two that we used

here are alkanethiolates on Au (7) and alkyl-siloxanes on  $\text{SiO}_2$  (9, 10). We chose the trifluoroacetoxy group ( $\text{CF}_3\text{CO}_2-$ ) as a probe for a number of reasons: (i) its surface concentration is easily measured by x-ray photoelectron spectroscopy (XPS) (11); (ii) it decomposes rapidly when irradiated with x-rays (6); (iii) it is easily introduced into SAMs (7, 8); and (iv) it is localized at the monolayer-air interface so that analysis of the concentration of F in the SAM is not complicated by the presence or generation of other signals.

In this report, we outline a study of the rate of damage to  $\text{CF}_3\text{CO}_2$  groups attached through an undecyl tether ( $\text{CF}_3\text{CO}_2-(\text{CH}_2)_{11}-$ ) to the surface of thin (50 to 200 Å) Si films supported on Au. We examined the relative rates of damage to the organic components of the system, the  $\text{CF}_3\text{CO}_2$ -terminated SAM, as a function of

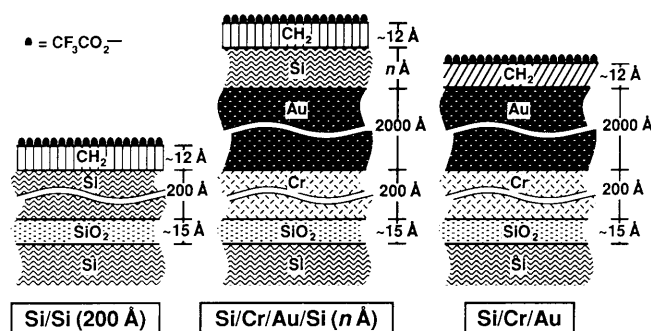


**Fig. 1.** Schematic illustration of the structures used in these studies. The lines denoting interfaces between materials are not meant to indicate that the interfaces are atomically flat; we have not measured their flatness. The lowest layers of Si represent Si(100) wafers ( $\sim 0.5$  mm thick) on which the assemblies were supported; the other layers of Si were prepared by evaporation and are probably amorphous. The evaporated films of Si contain a layer of  $\text{SiO}_2$  (not shown) of undetermined thickness (but probably  $\sim 15$  Å). Cr was used as an adhesion layer between the Si wafer and Au.

intensities of x-ray photons and of electrons. The results provide direct experimental confirmation that, under conditions relevant to technologies such as x-ray photolithography, electrons are responsible for most of the damage in one representative organic system. The electrons measured in this study include primary (photo- and Auger) and secondary electrons; we refer to these collectively as electrons.

To vary the number of electrons generated by interaction of the x-rays with the support, we prepared composite substrates (Fig. 1) comprising materials, Au and Si, characterized by very different electron yields upon x-ray irradiation. Au produces a higher electron yield than Si (11). To generate a range of intensities of electrons at the  $\text{CF}_3\text{CO}_2$  group, we coated thick films of Au ( $\sim 2000$  Å) with various thicknesses of evaporated Si (50, 100, and 200 Å as determined in situ with a quartz crystal microbalance; each  $\pm 10\%$ ). X-rays are not significantly attenuated by these thicknesses of Si (4), and the number of x-ray photons in the Au films—and thus the number of x-ray-induced photoelectrons from the Au—is similar in all of these samples. The electrons generated in the Au are, however, strongly scattered by the Si.

We confirmed the structure of the substrates with Rutherford backscattering spectroscopy (RBS) (12), using 3-MeV  $\text{He}^{2+}$  for independent characterization of the thickness of the Si overlayer. Figure 2 shows representative spectra; the signals associated with Si (inset) were analyzed (13) and thicknesses of 50, 105, and 185 Å (values estimated to be  $\pm 10$  Å) were inferred for the three samples. The width of the peak associated with Au suggests the reproducibility of the thicknesses of the multilayer substrates we fabricate ( $\sim \pm 10\%$ ). The spectra confirm that neither Cr nor bulk Si are localized at the substrate-vacuum interface. The RBS lacked the sensitivity to determine whether Au or Si was present at the surface. The films coated with Si exhibited no peaks

Department of Chemistry, Harvard University, Cambridge, MA 02138.

\*To whom correspondence should be addressed.

due to Au by XPS (only peaks attributable to Si, C, and O) and were unreactive to alkanethiols (14). These observations suggest that the Si layers are essentially free of pinholes.

The surfaces were derivatized by the self-assembly technique (7–9). SAMs were formed on the substrates exposing SiO<sub>2</sub> by reaction with CH<sub>2</sub>=CH(CH<sub>2</sub>)<sub>9</sub>SiCl<sub>3</sub> in hexadecane; the resulting olefin surfaces were transformed into trifluoroacetate surfaces through a two-step procedure in which BH<sub>3</sub>-H<sub>2</sub>O<sub>2</sub> and trifluoroacetic anhydride (TFAA) were used (8). SAMs were formed on Au by reaction with HS(CH<sub>2</sub>)<sub>11</sub>OH in deoxygenated absolute ethanol; the alcohol surface was converted to the trifluoroacetate by 30-s exposure to 5% TFAA-hexanes.

The XPS spectra of representative derivatized substrates (Fig. 3) show that the electron flux through the SAMs decreased as the thickness of the Si overlayer increased. Although peaks directly attributable to Au were not observed when the Si overlayer was  $\geq 50$  Å, we believe that the photoelectrons emitted from Au were, after inelastic

collisions, largely responsible for the increased baseline (relative to pure Si) for the samples containing an overlayer of Si. A 200-Å overlayer of Si virtually masked the presence of the underlying Au: the spectra of this system and that having only Si as substrate are very similar. The intensity of the F(1s) peak from the CF<sub>3</sub>CO<sub>2</sub> groups of the SAMs on the various substrates were approximately equal (Fig. 3); the different methods of forming SAMs generated approximately equal numbers of CF<sub>3</sub>CO<sub>2</sub> groups per unit area of surface (15).

The samples were exposed to a constant flux of monochromatized Al K<sub>α</sub> x-rays (1486.6 eV, anode power = 200 W) in a Surface Science X-100 XPS spectrometer (operating pressure  $\approx 10^{-9}$  torr); the spot size was  $\sim 1$  mm<sup>2</sup>. Electrons emitted from the F(1s) were detected with a concentric hemispherical analyzer (pass energy = 100 eV).

Figure 4 summarizes the relative intensity of the F(1s) peak on exposure of the

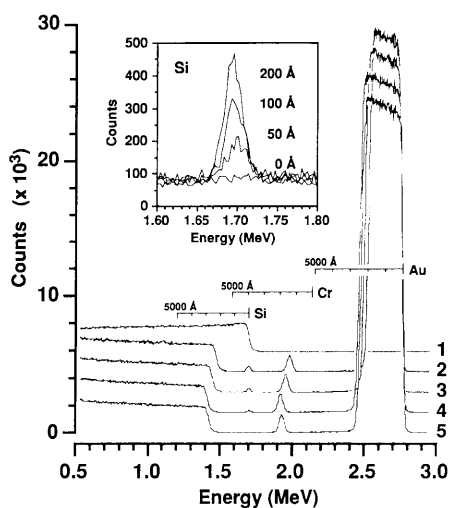


**Fig. 2.** RBS spectra of Si/Cr/Au/Si substrates for different thicknesses of the Si overlayer using 3-MeV He<sup>2+</sup>. The substrates were prepared by the sequential evaporation onto the surface of a Si wafer [Si(100) with  $\sim 15$  Å of native oxide] of 200 Å of Cr, 2000 Å of Au, and  $n$  Å ( $n = 0, 50, 100, \text{ or } 200$ ) of Si. The nominal thicknesses were determined with a quartz crystal microbalance (QCM) in the evaporator chamber. Quantitation of the signals associated with the Si layer (inset) yielded values of its thickness (error estimated to be  $\pm 10\%$ ): QCM (RBS) 50 Å (50 Å); 100 Å (105 Å); 200 Å (185 Å). The spectrum of Si is provided for comparison. The markers illustrate the location of a particular element relative to the air interface; for example, Cr is located  $\sim 2000$  Å beneath the surface. The assignment of signals is Au, 2.4 to 2.8 eV; Cr, 1.9 to 2.0 eV; Si, 1.7 eV, and the plateaus for energy  $E \leq 1.7$  eV. The spectra are displaced vertically for clarity. 1, Si/Si (200 Å); 2, Si/Cr/Au/Si (200 Å); 3, Si/Cr/Au/Si (100 Å); 4, Si/Cr/Au/Si (50 Å); and 5, Si/Cr/Au.

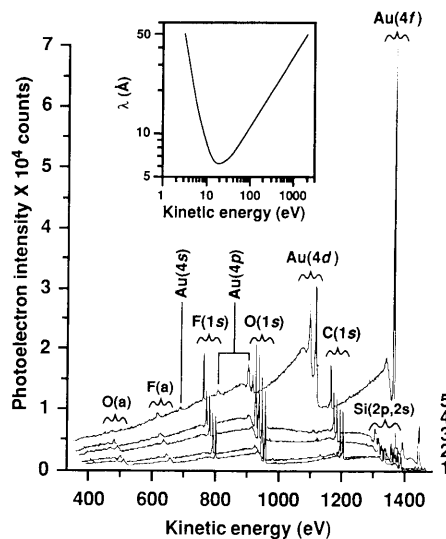


**Fig. 3.** XPS spectra of CF<sub>3</sub>CO<sub>2</sub>-terminated monolayers on Si/Cr/Au/Si substrates. The spectra were obtained on spots that had been previously unexposed to x-rays and required  $\sim 15$  min of exposure to the beam; the amount of damage to the SAM during this exposure is small ( $< 5\%$ ). Each spectrum has been offset horizontally by  $\sim 10$  eV from the one below it for clarity; the spectra have not been offset vertically. There is no residual Au signal even in the thinnest Si film (50 Å), and thus, we believe, no pinholes. This conclusion is reinforced by other experiments reported in the text. The hydrobroration procedure incorporated a contaminant, Ca (KE  $\approx 1100$  eV), that is present in  $< 1\%$  by atom. As we compare the rate of damage to photoelectron yield, presence of an impurity of Ca is not important. (Inset) The “universal” curve (11). The inelastic mean free path,  $\lambda$ , is defined as the distance at which the probability an electron traversing a medium without significant energy loss is  $1/e$ .  $1/\lambda$  is directly related to the probability of an electron interacting inelastically with a medium. The substrates (1–5) are defined in the legend to Fig. 2.

CF<sub>3</sub>CO<sub>2</sub>-terminated monolayers on the various substrates to Al K<sub>α</sub> x-rays. The intensity of the peak was measured during sequential 4-min intervals. With continued exposure to x-rays, the intensity of the F(1s) peak decreased. The amount of loss of F from the various substrates exposed to common numbers of photons is different (Fig. 4A); the loss of F is faster on the substrates that exhibit greater intensities of electrons upon irradiation with x-rays (Fig. 3). The different amounts of damage that occur upon exposing identical monolayers on substrates with different electron yields to a common intensity of x-rays demonstrate that electrons are, at some level, important in causing x-ray-induced damage.

The relative importance of photons and electrons in causing damage to the SAMs

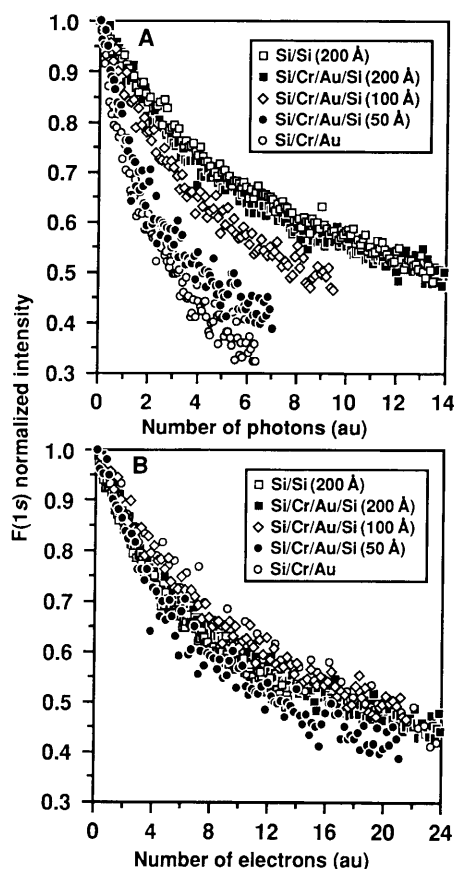


**Fig. 4.** X-ray-induced damage to CF<sub>3</sub>CO<sub>2</sub>-terminated monolayers on Si/Cr/Au/Si substrates as a function of (A) the number of photons and (B) photoelectrons to which the CF<sub>3</sub>CO<sub>2</sub> group were exposed. The intensity of the F(1s) signal was determined from sequential scans ( $\sim 4$  min each). We estimated the number of electrons from these samples by integrating (16, 17) the XPS spectra in Fig. 3. In (B), the substrates require different lengths of exposure to the x-ray beam to yield similar numbers of electrons. The different rates of loss evidenced in the upper panel and the similarity of the profiles in (B) suggest that the damage to the SAMs results primarily from the electrons and not from the photons interacting with the SAMs.

can be estimated from the data in Fig. 3. The flux of electrons from the various substrates under a common flux of photons is different. We have estimated the relative intensities of electrons from the substrates by integrating (16, 17) the XPS spectra in Fig. 3 over the kinetic energy (KE) range from 387 to 1487 eV. We are limited by the electrostatic analyzer on the XPS to quantitation of electrons of KE  $\geq$  400 eV, and there may be systematic errors in estimating the relative intensities of electrons in the range of energies that are most damaging ( $\sim$ 50 eV) from the observed yield of electrons of energies  $>$ 400 eV (17, 18). In Fig. 4B, we plot the intensity of F(1s) from the various substrates versus the number of electrons to which the SAM was exposed. In order to generate similar doses of electrons, we exposed the samples containing thicker overlayers of Si to the x-ray beam longer than those having thinner overlayers. The profiles in Fig. 4B are remarkably similar (especially given that the substrates had different lengths of exposure to the x-ray beam) and suggest that the primary and secondary electrons are much more important in the damage process than are the x-ray photons. We believe the deviations present are primarily due to difficulties in maintaining a constant photon flux.

Although the data do not determine whether electrons are solely responsible for causing damage, they are, however, consistent with the finding that primary and secondary electrons are responsible for most (and maybe all) of the damage to a representative organic system upon irradiation with x-rays.

- distance required to reduce the probability an electron escaping to  $1/e$ ) through a material to the kinetic energy of the electron [M. P. Seah and W. A. Dench, *Surf. Interface Anal.* **1**, 2 (1979)].
11. J. H. Scofield, *J. Electron Spectrosc. Relat. Phenom.* **8**, 129 (1976).
  12. L. C. Feldman and J. W. Mayer, *Fundamentals of Surface and Thin Film Analysis* (Elsevier Science, New York, 1986), chaps. 2 and 3.
  13. The RBS spectra were analyzed with Spectrum Analysis (SA), a PC version of the TEK program for RBS analysis developed at Oak Ridge National Laboratory. SA was written by P. M. Smith (Division of Applied Sciences, Harvard University, Cambridge, MA, 1989).
  14. We tested the presence of Au at the surface of the Si/Cr/Au/Si substrates by immersing the Si-coated Au substrates in a 1 mM ethanolic solution of a F-containing alkanethiol [ $\text{CF}_3\text{CF}_2\text{CH}_2\text{O}(\text{CH}_2)_{11}\text{SH}$ ] overnight. Thiols react with soft metal-metal oxides, such as Au, but do not react with hard metal-metal oxides, such as  $\text{Al}_2\text{O}_3$  or  $\text{SiO}_2$  [P. E. Laibinis, J. J. Hickman, M. S. Wrighton, G. M. Whitesides, *Science* **245**, 845 (1989); P. E. Laibinis and G. M. Whitesides, unpublished results]. No F was detected on any substrate exposing Si by XPS, suggesting that the Si-coated Au substrates reveal no (or very little) Au at their surface. We estimate that we would have detected 0.1% of a monolayer of the fluorinated thiolate.
  15. We have estimated that the procedure used to derivatize Si yields  $\sim$ 80% of the number of  $\text{CF}_3\text{CO}_2$

- groups as the procedure used to derivatize Au (8).
16. In estimating the relative flux of electrons from the various substrates, the spectra (Fig. 3) were corrected for differences in the efficiency of the electrostatic analyzer with the KE of the electron. The effect of this correction on the relative electron flux is small ( $<$ 2%).
  17. We have also analyzed the XPS spectra incorporating differences in the likelihood of an electron to interact with the SAM (estimated as  $1/\lambda$ ) and find that the correction would be small ( $\leq$ 3%); the direction of this correction is opposite that due to detector inefficiencies (16).
  18. M. P. Seah and G. C. Smith, *Surf. Interface Anal.* **15**, 751 (1990).
  19. Supported in part by the Office of Naval Research, the Defense Advanced Research Projects Agency, and the National Science Foundation (grant CHE-88-12709). XPS and RBS spectra were obtained with instrumental facilities purchased under the Defense Advanced Research Projects Agency and University Research Initiative Program and maintained by the Harvard University Materials Research Laboratory. We thank J. F. Chervinsky and P. M. Smith for help in characterizing the substrates by RBS, J. P. Folkers for supplying the  $\text{H}_2\text{C}=\text{CH}(\text{CH}_2)_6\text{SiCl}_3$ , C. D. Bain for discussions and suggestions, and S. M. Bonser, J. P. Folkers, and J. P. Mathias for critical readings of this manuscript.

29 May 1991; accepted 30 August 1991

#### REFERENCES AND NOTES

1. D. R. Wheeler and S. V. Pepper, *J. Vac. Sci. Technol.* **20**, 226 (1982); C. P. Buchwalter and G. Czornyji, *ibid.* **A 8**, 781 (1990).
2. W. M. Moreau, *Semiconductor Lithography: Principles, Practices and Materials* (Plenum, New York, 1987), pp. 104-111.
3. W. Schnabel and H. Sotobayashi, *Prog. Polym. Sci.* **9**, 297 (1983).
4. For example, the penetration depth of x-rays (KE  $\sim$ 2 keV) into organic materials is of the order of micrometers; of electrons, it is of the order of  $\sim$ 100 Å [M. P. Seah, in *Practical Surface Analysis*, D. Briggs and M. P. Seah, Eds. (Wiley, Chichester, 1983), chap. 5]. In our experiment, we estimate the flux of x-ray photons experienced by the  $\text{CF}_3\text{CO}_2$ -group to be more than  $\sim$ 100 times greater than the flux of electrons.
5. C. J. Powell and M. P. Seah, *J. Vac. Sci. Technol. A* **8**, 735 (1990).
6. C. D. Bain, thesis, Harvard University (1988).
7. R. G. Nuzzo and D. L. Allara, *J. Am. Chem. Soc.* **105**, 4481 (1983); C. D. Bain and G. M. Whitesides, *Angew. Chem. Int. Ed. Engl.* **101**, 522 (1989), and references therein; G. M. Whitesides and P. E. Laibinis, *Langmuir* **6**, 87 (1990), and references therein.
8. S. R. Wasserman, Y.-T. Tao, G. M. Whitesides, *Langmuir* **5**, 1074 (1989).
9. A. Ulman, *An Introduction to Ultrathin Organic Films* (Academic Press, Boston, 1991), pp. 245-279.
10. The "universal" curve (Fig. 3, inset) relates the inelastic mean free path of an electron,  $\lambda$  (the